VOLUME 121, NUMBER 23
JUNE 16, 1999

JOURNAL OF THE AMERICAN CHEMICAL SOCIETY

Elucidation of Mechanism of Inhibition and X-ray Structure of the TEM-1 β-Lactamase from *Escherichia coli* Inhibited by a *N*-Sulfonyloxy-β-lactam

Peter Swarén,[†] Irina Massova,[‡] John R. Bellettini,[§] Alexey Bulychev,[‡] Laurent Maveyraud,[†] Lakshmi P. Kotra,[‡] Marvin J. Miller,[§] Shahriar Mobashery,*[,‡] and Jean-Pierre Samama*[,†]

Contribution from the Groupe de Cristallographie Biologique, Institut de Pharmacologie et de Biologie Structurale du CNRS, 205 route de Narbonne, 31077-Toulouse Cedex, France, Department of Chemistry, Wayne State University, Detroit, Michigan 48202, and Department of Chemistry and Biochemistry, University of Notre Dame, Notre Dame, Indiana 46556

Received February 8, 1999

Abstract: Class A β-lactamases are inactivated by a novel type of monocyclic β-lactams described recently (*J. Am. Chem. Soc*. **1995**, *117*, 5938). A compound of this class, (±)-*trans*-1-*N*-(tosyloxy)-3-(1-hydroxyethyl)-4-phenyl-2-azetidinone, is synthesized, is shown to acylate the active site of the TEM-1 β-lactamase from *Escherichia coli* rapidly, and resists deacylation for several days. The crystal structure of the enzyme−inhibitor complex was determined at 1.95 Å resolution. The features of the three-dimensional structure of this acyl−enzyme species and mechanistic studies revealed that a fragmentation of the inactivator ensued on acylation of the active-site serine and that the ester carbonyl oxygen was outside the oxyanion hole. This ester carbonyl makes a strong hydrogen bond to the protonated form of the side chain of Glu-166, the general base for deacylation of the typical acyl−enzyme intermediates in the normal catalytic process. Furthermore, interactions within the active site mandated the existence of the former β-lactam amine as an imine or a ketone, and not as an enamine or an enol, and shed light on the unique mechanism of action of these enzyme inactivators. This type of inactivator holds the promise of application for inhibition of other enzymes.

The hydrolytic action of β-lactamases is the primary cause of bacterial resistance to β-lactam antibiotics.[1−4] These enzymes have been selected to be present in many pathogens, and the use of a wide range of these antibiotics in the clinic has facilitated evolution of the enzymes for expression of many phenotypic resistance profiles.[1−4] There are over 250 known β-lactamases, of which one group, the class A enzymes, are the most common.[3] In light of their prevalence, inhibitors of class A β-lactamases are highly sought, and three such inhibitors, clavulanic acid, sulbactam, and tazobactam,[3] have been introduced to the clinic. However, an increasing number of variants of β-lactamases resistant to the inhibition process have been identified since 1992.[5] It has been demonstrated that the mechanism of inactivation of these enzymes by all three

[†] Institut de Pharmacologie et de Biologie Structurale du CNRS.
[‡] Wayne State University.
[§] University of Notre Dame.

(1) Massova, I.; Mobashery, S. *Antimicrob. Agents Chemother*. **1998**, *42*, 1.
(2) Medeiros, A. A. *Clin. Infect. Dis*. **1997**, *24* (Suppl 1), S19.
(3) Bush, K.; Mobashery, S. In *Resolving the Antibiotic Paradox: Progress in Understanding Drug Resistance and Development of New Antibiotics*; Rosen, B. P., Mobashery, S., Eds.; Plenum Press: New York, 1998; pp 71−98.
(4) Bush, K.; Jacoby, G. A.; Medeiros, A. A. *Antimicrob. Agents Chemother*. **1995** *39*, 1211. Matagne, A.; Lamotte-Brasseur, J.; Frére, J. M. *Biochem. J.* **1998**, *330*, 581.

10.1021/ja990400q CCC: $18.00
Published on Web 05/27/1999

compounds is similar,[6] and variants of these enzymes may thus evolve, which would, in principle, give cross-resistance to all three inactivators.[5] Therefore, new β-lactamase inhibitors that function by distinct mechanisms are highly desirable.

We have reported our findings on a novel class of monobactam inhibitors for class A β-lactamases.[7] These molecules have the general structure shown below (**1**). This class of compounds distinguishes itself in its ability to inactivate the enzyme exceedingly rapidly. Compound **2**, a prototype inhibitor

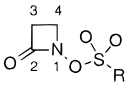

1

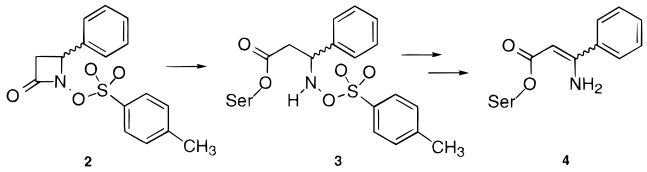

2 **3** **4**

of this kind, acylates the active site of the enzyme in seconds. The immediate acylated species (**3**) undergoes rearrangement to give the inhibited species (**4**), following the release of the good leaving group. Recovery of the enzyme activity occurred within 2−3 h, and we suggested that this species resists deacylation in light of the fact that it is an α,β-unsaturated ester.

In this report, we have explored the details of the mechanism of action of this type of enzyme inhibitors by kinetics measurements and X-ray structure determination of the TEM-1 β-lactamase−inhibitor complex. The study was aided by the design and synthesis of inactivator **5** that resists deacylation from the

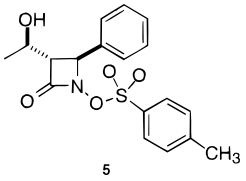

5

active site of the enzyme for several days. This inactivator was used to modify the TEM-1 β-lactamase from *Escherichia coli*, the parent enzyme of a group of 69 class A β-lactamases (as of May 1999). The crystal structure of the complex is described herein, which helped elucidate the mechanism of action of the inactivator.

Scheme 1

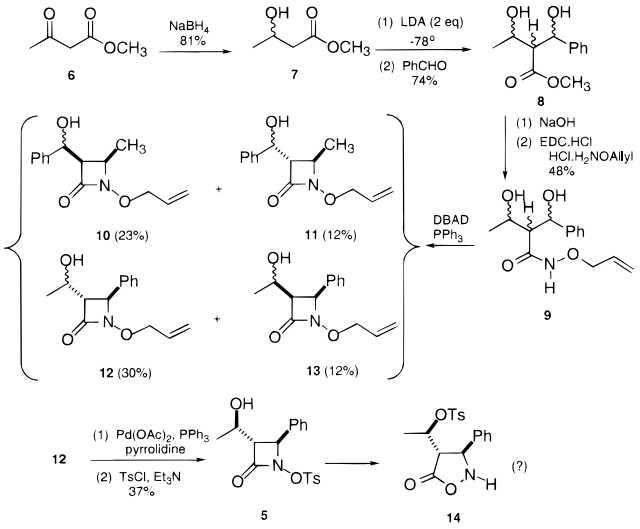

Results and Discussion

One of the best inhibitors of this class that we had studied previously was compound **2**. This compound modified the active site Ser-70 of the TEM-1 β-lactamase rapidly [$k_{inact}/K_i = (1.12 \pm 0.08) \times 10^4$ M^{-1} s^{-1}].[7] To stabilize the acyl−enzyme intermediate and thus improve the inhibitory properties, we incorporated the hydroxyethyl group in the structure of inactivator **2** to arrive at compound **5**. Indeed, earlier work by others[8] and by us[9,10] had indicated that the presence of the 1(*R*)-α-hydroxyethyl group adjacent to the lactam carbonyl of other classes of β-lactams imparted substantial stability to the acyl−enzyme species. The magnitude of this effect on turnover kinetic parameters could be as much as 50 000-fold,[9] and the effect stems from the stereoelectronic interactions of 1(*R*)-α-hydroxyethyl group within the active site. Compound **5** was therefore expected to resist strongly the deacylation process.

Scheme 1 shows the synthesis for compound **5**. The synthesis commenced with the reduction of methyl acetoacetate (**6**) by sodium borohydride in methanol to afford methyl 3-hydroxybutanoate (**7**) in 71% yield. Treatment of **7** with 2 equiv of LDA, to form the dianion, followed by the addition of benzaldehyde afforded a mixture of diastereomeric aldol products **8** (four diastereomers as a 39:33:24:4 mixture) in 74% yield. Saponification of the methyl esters of the mixture of diastereomers using 1.0 M NaOH afforded the corresponding carboxylic acids, which were coupled with *O*-allylhydroxylamine using the water-soluble carbodiimide EDC-HCl to affordhydroxamates **9** in 48% yield. The mixture was used directly in the next step. The β-hydroxy hydroxamates were cyclized to the corresponding β-lactams using Mitsunobu conditions[11] in the presence of di-*tert*-butyl azodicarboxylate (DBAD) and triphenylphosphine (PPh_3) to afford a diastereomeric mixture of four β-lactams, which were separated by column chromatography to obtain the pure isomers **10**−**13**. Only the relative stereochemistry at the hydroxyl bearing carbon of

(5) Vedel, G.; Belaaouaj, A.; Gilly, L.; Labia, R.; Philippon, A.; Névot, P.; Paul. G. *J. Antimicrob. Chemother*. **1992**, *30*, 449. Blazquez, J.; Baquero, M. R.; Canton, R.; Alos, I.; Baquero, F. *Antimicrob. Agents Chemother*. **1993**, *37*, 2059. Belaaouaj, A.; Lapoumeroulie, C.; Canica, M. M.; Vedel, G.; Névot, P.; Krishnamoorthy, R.; Paul. G. *FEMS Microbiol. Lett*. **1994**, *120*, 75. Farzaneh, S.; Chaibi, E. B.; Peduzzi, J.; Barthelemy, M.; Labia, R.; Blazquez, J.; Baquero, F. *Antimicrob. Agents Chemother*. **1996**, *40*, 2434. Bret, L.; Chaibi, E. B.; Chanal-Claris, C.; Sirot, D.; Labia, R.; Sirot, J. *Antimicrob. Agents Chemother*. **1997**, *41*, 2547. Bermudes, H.; Jude, F.; Arpin, C.; Quentin, C. *Antimicrob. Agents Chemother*. **1997**, *41*, 222. Canica, M. M.; Lu, C. Y.; Krishnamoorthy, R.; Paul, G. C. *J. Mol. Evol*. **1997**, *44*, 57. Sirot, D.; Recule, C.; Chaibi, E. B.; Bret, L.; Croize, J.; Chanal-Claris, C.; Labia, R.; Sirot, J. *Antimicrob. Agents Chemother*. **1997**, *41*, 1322. Canica, M. M.; Caroff, N.; Barthelemy, M.; Labia, R.; Krishnamoorthy, R.; Paul, G.; Dupret, J. M. *Antimicrob. Agents Chemother*. **1998**, *42*, 1323. Vakulenko, S. B.; Geryk, B.; Kotra, L. P.; Mobashery, S.; Lerner, S. A. *Antimicrob. Agents Chemother*. **1998**, *43*, 1542. A Web site gives updated information on β-lactamases and their clinical variants: http://www.lahey-.org/studies/webt.htm.

(6) Massova, I.; Mobashery, S. *Acc. Chem. Res*. **1997**, *30*, 162.

(7) Bulychev, A.; O'Brien, M. E.; Massova, I.; Teng, M.; Gibson, T. A.; Miller, M. J.; Mobashery, S. *J. Am. Chem. Soc*. **1995**, *117*, 5938.

(8) Cama, L. D.; Wildonger, K. J.; Guthikonda, R.; Ratcliffe, R. W.; Christensen, B. G. *Tetrahedron* **1983**, *39*, 2513. Cama, L.; Christensen, B. G. *J. Am. Chem. Soc*. **1978**, *100*, 8006. Shih, D. H.; Hannah, J.; Christensen, B. G. *J. Am. Chem. Soc.* **1978**, *100*, 8004. Iwata, H.; Tanaka, R.; Ishiguro, M. *J. Antibiot*. **1990**, *43*, 901. Murakami, M.; Aoki, T.; Matsuura, M.; Nagata, W. *J. Antibiot*. **1990**, *43*, 1441.

(9) Taibi, P.; Mobashery, S. *J. Am. Chem. Soc*. **1995**, *117*, 7600.

(10) Miyashita, K.; Massova, I.; Mobashery, S. *Bioorg. Med. Chem. Lett*. **1996**, *6*, 319.

(11) Miller, M. J. *Acc. Chem. Res*. **1986**, *19*, 49.

the hydroxyethyl side chain of each compound could not be assigned unambiguously. The stereochemistry of compound **5** at that site was assigned from the interactions observed in the X-ray structure of compound **5** in the TEM-1 β-lactamase complex. We thought that complexation of phosphorus with diol **9** would possibly allow for some selectivity for cyclization at the benzylic position over the secondary position; however, this selectivity was not observed. The regiochemistry of the cyclization products was determined using 2-D COSY NMR experiments. In compounds **10** and **11**, the proton that is coupled to the hydroxyl proton showed coupling with the C-3 hydrogen of the β-lactam ring. In contrast, in compounds **12** and **13**, the proton coupled to the hydroxyl proton showed coupling with the methyl group on the C-3 substituent in addition to the C-3 hydrogen of β-lactam ring. The stereochemistry on the β-lactam ring was determined from the coupling constants of the C-3 and C-4 protons on the ring. The stereochemistry of the site of attachment of the hydroxyl group could not be determined at this stage. β-Lactam **12** was allowed to react with palladium diacetate [$Pd(OAc)_2$] and triphenylphosphine in the presence of pyrrolidine (as the allyl cation scavenger) to afford the *N*-hydroxy β-lactam, which was treated with *p*-toluenesulfonyl chloride in the presence of triethylamine to afford *N*-tosyloxy β-lactam **5** in 37% yield. We noticed that, after approximately 3 days of storage of β-lactam **5** at room temperature, it was contaminated with a rearrangement product, which we attribute to structure **14**, although the structure assignment is equivocal. If our notion for the structure of this rearrangement product is correct, the tosylate group may first transfer to the free hydroxyl group, and then the resulting *N*-hydroxy β-lactam may undergo a known rearrangement[12] to afford **14**.

Compound **5** inactivated the TEM-1 β-lactamase rapidly. The rate of this process could not be attenuated effectively in competition with substrates to permit evaluation of individual parameters for enzyme inhibition. However, we have used three parameters in evaluation of the kinetic properties of this compound with this enzyme. The second-order rate constant for inactivation (k_{inact}/K_i) was assessed for the inactivation process; the larger the number, the faster the process. This parameter was evaluated at $(3.20 \pm 0.15) \times 10^3\ M^{-1}\ s^{-1}$. The partition ratio ($k_{cat}/k_{inact}$) was evaluated to be 7, which is an expression of the efficiency of the inactivation process; that is to say, seven molecules were hydrolyzed before the onset of enzyme inactivation. We evaluated the ease for recovery of activity (k_{rec}), as a measure of the longevity for the inactive enzyme species; the smaller this rate constant, the better the inactivator. As expected, we observed exceedingly slow deacylation for the inactivated enzyme complex, and the recovery of activity was biphasic. A relatively rapid phase accounting for only 8% of the recovery of activity could be discerned only in the presence of high concentrations of substrates (not seen in Figure 1) and proceeded with a rate constant comparable to those for the other monobactams of this type [$k_{rec} = (1.6 \pm 0.4) \times 10^{-3}\ s^{-1}$]. However, the slower phase for deacylation took place over a remarkably long period of several days (Figure 1), which incidentally allowed for recovery of no more than 15% of activity in 6 days [$k_{rec} = (1.3 \pm 0.2) \times 10^{-5}\ s^{-1}$]. The rate differential for the two phases of the recovery of activity is over 120-fold. As will be described subsequently in this manuscript, there are two acyl−enzyme species for the inhibited complex. One is an immediate acyl−enzyme species with the ester carbonyl housed in the active-site oxyanion hole, and the other

(12) Zercher, C. K.; Miller, M. J. *Tetrahedron Lett.* **1989**, *30*, 7009. Hirose, T.; Chiba, K.; Mishio, S.; Nakano, J.; Uno, H. *Heterocycles* **1982**, *19*, 1019.

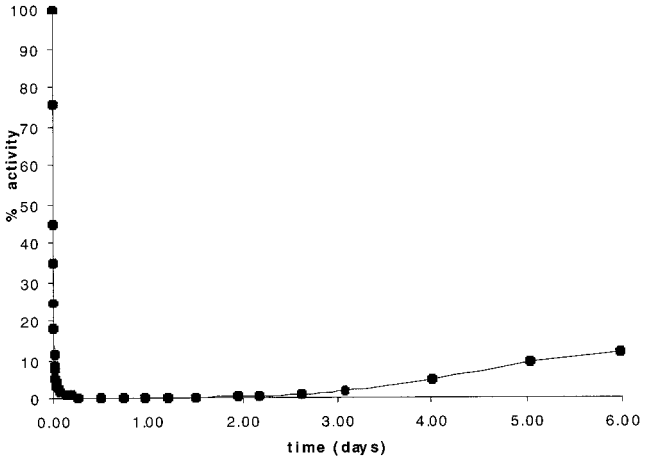

Figure 1. Activity profile of the TEM-1 β-lactamase as a function of time in the presence of compound **5**.

(seen in the X-ray structure) has the ester carbonyl displaced from the oxyanion hole. We suggest that the first, the immediate acyl−enzyme species, is the one that gives the more rapid rate constant for deacylation, and the other, the one with the carbonyl out of the oxyanion hole, accounts for the slower step for deacylation.

The monobactam inactivators are recognized by the TEM-1 β-lactamase, whereby they form a noncovalent preacylation complex. Enzyme acylation takes place rapidly to give the immediate acylated species (such as **3**), and a species such as **4** would account for enzyme inactivation.[7] We noted that, on inactivation of the enzyme by compounds **2** and **5**, the tosylate was eliminated quantitatively but that no chromophore formation was seen with compound **5**, in contrast to compound **2**.

Structures **15**−**18** show the possibilities for the nature of the acyl−enzyme species of the TEM-1 β-lactamase with compound**5**. The atoms of structures **15** and **17** are numbered

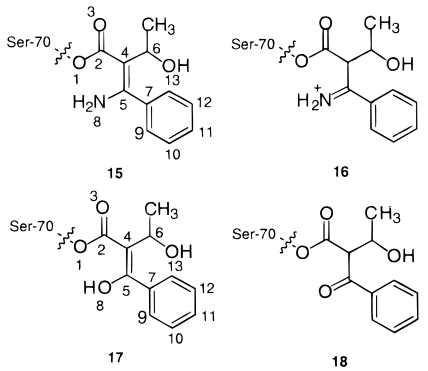

arbitrarily (atoms 1−13). In light of the fact that the chromophore at 276 nm for the α,β-unsaturated ester[7] was not seen with the use of compound **5**, we concluded that structures **15** and **17** may be unlikely. Hydrolysis of the iminium group of **16**, the immediate product of the loss of the leaving group, would generate **18**, and either **16** or **18** may account for the collective data for experiments in solution. These species are simply tautomers of **15** and **17**, respectively.

Crystals of the inactivated enzyme, produced by soaking the native TEM-1 β-lactamase crystals with inhibitor **5**, were sensitive to X-ray exposure. Crystals diffracted weakly when data collection was performed at −10 °C, but the diffraction pattern was much improved when crystals were flash-cooled at 100 K. A 1.95 Å data set was collected under these conditions (Table 1; Experimental Section). Crystals belonged to the space

Table 1. Data Processing and Refinement Statistics

	overall resolution range 35.0−1.95	highest resolution shell 2.00−1.95
no. of observns	48398	3636
no. of ind reflns	14329	1122
completeness (%)	88.0	96.4
R_{merge}[a]	0.043	0.082
$\langle I/\sigma I\rangle$	24.9	16.1

R_{factor}: 0.206 R_{free}: 0.258
2014 protein atoms ($\langle B\rangle = 19.5$ Å^2) 349 solvent atoms ($\langle B\rangle = 32.1$ Å^2)
rms deviation
bond length: 0.015 Å bond angles: 1.3°
dihedral angles: 21.8° improper angles: 0.75°

[a] $R_{merge} = \Sigma\Sigma|\langle I\rangle - I_i|/\Sigma\Sigma I_i$.

group $P2_12_12_1$, with cell parameters $a = 40.94$ Å, $b = 59.31$ Å, and $c = 87.58$ Å.

The first cycles of refinement, which included a rigid body optimization as the initial step, were performed using reflections from 20 to 1.95 Å and the native TEM-1 β-lactamase structure as the initial model. The R_{factor} and the R_{free} values dropped from 0.55 to 0.23 and from 0.56 to 0.29, respectively. The electron density maps computed at this stage showed a continuous electron density in the active site extending from Ser-70 O_γ, which indicated binding of the inactivator as an acyl−enzyme complex. In the last rounds of refinement, the significant electron densities found in the oxyanion hole and in the vicinity of Arg-244 were assigned as a water molecule and a sulfate ion, respectively. Atoms of the inhibitor were introduced at this stage. All protein atoms, except a few solvent-exposed side chains, were visible in the final electron density map, which allowed inclusion of 349 water molecules and one sulfate ion. The final R_{factor} was 0.206 ($R_{free} = 0.258$) for all reflections between 20 and 1.95 Å (Table 1).

Electron density beyond atom 5 of the inactivator bound in the active site was present from the first step of refinement. However, it did not significantly improve in the next steps in order to allow an unambiguous model building of the atom at position 8 and of the phenyl group. Such an observation is usually interpreted to be the result of the motion of the chemical groups. This clearly applies to our case, as will be elaborated below.

The protein structure in the complex is very similar to the structure of the native enzyme. A global superimposition of both structures based on the main-chain atoms led to a rms deviation of 0.4 Å. Atoms O_1 (Ser-70 O_γ), C_2, O_3, C_4, and C_6 of the inhibitor and the hydroxyl and methyl substituents on C6 are common to the four plausible species that may account for inhibition of the enzyme (structures **15**−**18**). The electron density showed that Ser-70 O_γ is acylated and that the ester oxygen atom O_3 is not in the oxyanion hole. The ester carbonyl has displaced the hydrolytic water molecule and is located at 2.8 Å from the O_{ϵ^1} oxygen atom of Glu-166, which indicates that the side-chain function of this amino acid should be protonated in the complex (Figure 2A and Scheme 2; the distances shown in the scheme for hydrogen bonds are for those between the two heteroatoms).

The structural constraints brought about by the planar character of the potential inactivated species **15** and **17** would bring the hydroxyl or the amino group, respectively, at atom position 8, to an unfavorable 2.0 Å distance from the side chain of Asn-170. The electron density of Asn-170 is well-defined, and according to the structure refinement, no alternate conformation for its side chain may be postulated. Hence, structures **15** and **17** cannot be accommodated by the information from the X-ray structure, consistent with the findings from the biochemical studies (discussed earlier). On the other hand, the electron density corresponding to the C_4-C_5 bond, to the C_7, C_9, and C_{13} atoms, and to the hydroxyl and methyl groups of the 6α substituent agree with the binding of species **16** and/or **18** to the protein. Based on hydrogen bond and van der Waals patterns, the stereochemistry at carbon 6 is *S*. The hydroxyl group is found at 2.7 Å from Ser-130 O_γ and the methyl group at 3.5 Å from the phenyl ring of Tyr-105.

The absence of a well-defined electron density corresponding to the iminium/ketone group and to the phenyl ring, the value of the refined occupancy of the bound inhibitor (0.74), the increasing mobility according to the temperature factors from atom 1 to 5 (20.2 to 36.9 Å^2), and the unusual sensitivity of the TEM crystals upon complex formation with compound **5** collectively suggest that the structure of the inhibited species in the crystal is not uniform. These observations would be in line with the coexistence of species **18** along with **16**, in the modified enzyme. The iminium moiety of **16** would be located at 2.4 Å to the main-chain oxygen atom of Ala-237 and at 2.9 Å to the O_{δ^1} atom of the Asn-170 side chain (Scheme 2). These interactions would not be compatible with the same binding of species **18**, which possesses an oxygen atom at position 8. A rotation about the C_4-C_5 bond, which is only possible for species **16** and **18**, likely explains the weak electron density for atoms beyond atom 5.

Despite acylation by the inhibitor, the TEM-1 enzyme still binds a water molecule in the oxyanion hole, at 2.9 and 2.4 Å to the main-chain nitrogen atoms of residues 70 and 237, respectively. In contrast to the inhibitor, this water molecule has the same occupancy (1.0) and temperature factor (15.2 Å^2) as the neighboring protein atoms. It occupies a position similar to that found in the unmodified enzyme. This observation indicates that, after acylation of Ser-70 by the inhibitor and the motion of the ester carbonyl out of the oxyanion hole, a water molecule moved in to reoccupy the void in the oxyanion hole. An interesting comparison could be made between the binding modes of the two acyl−enzyme intermediates of imipenem (a carbapenem antibiotic) and of compound **5**.[13] In the X-ray structure of the TEM−imipenem complex, the carbonyl ester was also found outside the oxyanion hole, but oriented toward Ser-130 O_γ. However, no water molecule was found in the oxyanion hole because of the dynamic motion of the oxygen atom of the carbonyl ester in and out of this site, as demonstrated by molecular dynamics simulations.[13] Such a dynamic situation does not appear to be the case for the inhibitory species of **5** seen in the X-ray structure. The tetrahedral electron density in the vicinity of Arg-244 was attributed to a sulfate ion supplied by the crystallization medium. It was located at 2.5−3.1 Å to the N_ζ atom of Lys-234, the O_γ atom of Ser-235, and the N_{η^2} of Arg-244. This region of the protein is characterized by a significant positive electrostatic potential and may provide, in solution, a binding site for the sulfonate moiety of **5** on its departure from the immediate acyl−enzyme intermediate. We hasten to add that the presence of the sulfate ion is not required for enzyme inactivation, since all of the kinetics experiments were performed in its absence.

A number of features about this inhibitor are novel. First, acylation of the active-site serine by our inactivator is driven by the highly favorable steric and electrostatic interactions of the inhibitor with the active-site functions. A key interaction

(13) Maveyraud, L.; Mourey, L.; Kotra, L. P.; Pedelacq, J.-D.; Guillet, V.; Mobashery, S. and Samama, J. P. *J. Am. Chem. Soc.* **1998**, *120*, 9748.

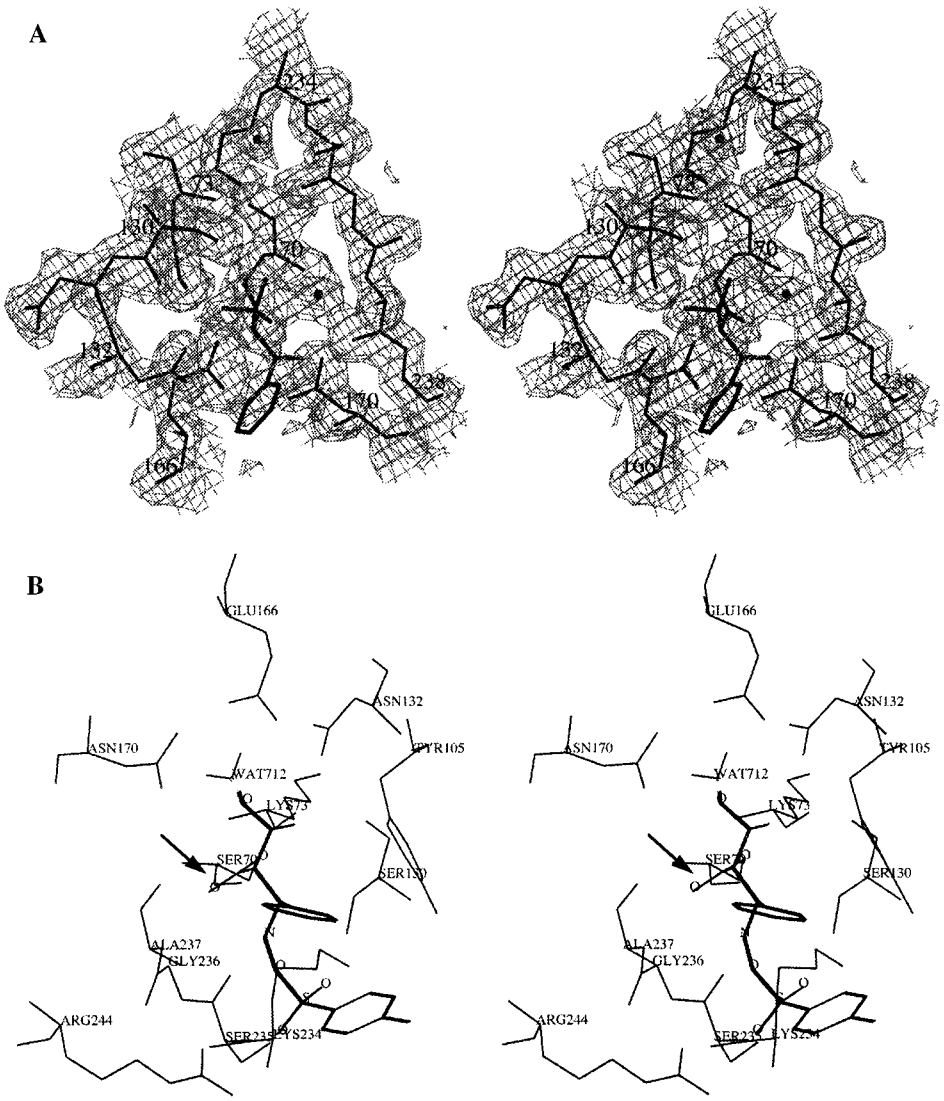

Figure 2. (A) Stereoview of the crystal structure of the TEM-1 β-lactamase from *E. coli* modified by **5**. The final $[3F_{obs} - 2F_{calc}, \Phi_{calc}]$ electron density map has been contoured at 1 σ (20−1.95 Å). (B) Stereoview of the energy-minimized structure for the immediate acyl−enzyme intermediate of compound **5** with the TEM-1 β-lactamase from *E. coli*. The arrow shows the carbonyl moiety of the acyl−enzyme intermediate. In the immediate acyl−enzyme intermediate (image B), the ester carbonyl occupies the oxyanion hole, and in the X-ray structure (image A), this moiety moved out of the oxyanion hole and a water molecule (shown as spheres at 3 o'clock) occupies this site.

Scheme 2

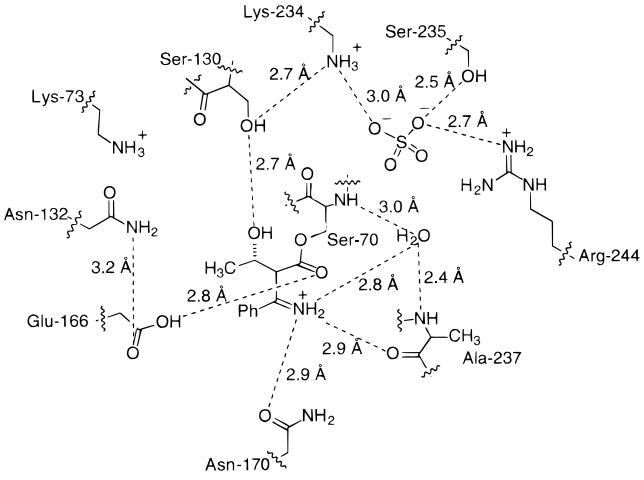

here is with the sulfonate of the inhibitor, which serves as a surrogate for the invariant carboxylates for typical substrates found in this position.[7] These interactions readily anchor the inhibitor in the active site. The immediate acyl−enzyme intermediate (Figure 2B) forms on acylation of Ser-70 and loses this good leaving group—the sulfonate—by either an α- or β-elimination process as discussed previously,[7] to give rise to the final inactivated species. The loss of the sulfonate moiety gives additional flexibility to the acyl−enzyme species, which rearranges into a new low-energy entity. This is the inactivated species that one sees in the crystal structure of the TEM-1 β-lactamase modified by **5**, which shows structural elements unique to this type of enzyme inactivation, and indeed is quite distinct compared to all known structures for inhibited β-lactamases.

As described earlier, the hydroxyethyl group in inactivator **5** was meant to prevent the early deacylation of the acyl−enzyme intermediate. Indeed, this moiety would play this role at the stage of the formation of the immediate acyl−enzyme species (Figure 2B). However, after the departure of the sulfonate group, the strong interactions it forms with the side chain of Ser-130 (Scheme 2 and Figure 2A) direct the oxygen of the ester moiety into the space that the hydrolytic water normally occupies, such that the water molecule is displaced from the active site. This

is the structural reason that imparts hydrolytic stability to this inhibited enzyme species. Compound **5** was synthesized as a racemic mixture. The *S*-stereogenicity at the atom position 6 was deduced from the polar and van der Waals interactions observed in the crystal. Modeling experiments were performed with both enantiomers at this position, as we were not certain of the absolute configuration before the crystal structure became available.

The type of monobactam inhibitor for β-lactamases reported herein operates by a mechanism entirely distinct from those of the clinically used inactivators. Whereas the chemistry described in this report was envisioned for β-lactamases, the principles disclosed should be of general application for any enzyme that operates by covalent catalysis.

Experimental Section

Melting points (mp's) were determined on a Thomas-Hoover capillary melting point apparatus in open capillaries and are uncorrected. Infrared (IR) spectra were obtained on a Perkin-Elmer 1420 IR spectrophotometer and were calibrated with the 1601 cm^{-1} band of polystyrene. Nuclear magnetic resonance (NMR) spectra were obtained on a General Electric GN-300, a Varian Unity Plus 300, or a Varian VXR500S spectrometer. ^1H NMR chemical shifts are reported in parts per million relative to tetramethylsilane (0.00 ppm). ^{13}C NMR spectra were referenced relative to the center peak of $CDCl_3$ (77.00 ppm). Fast-atom bombardment (FAB, xenon, 3-nitrobenzyl alcohol matrix) mass spectra were obtained on a JEOL JMS-AX505HA mass spectrometer. Thin-layer chromatography (TLC) was conducted on silica gel 60 F_{254} (0.2 mm thickness, aluminum support), and the chromatograms were visualized with ultraviolet light and by dipping in 10% phosphomolybdic acid (PMA) in ethanol, followed by heating. Flash column chromatography was performed using silica gel 60 (EM Science, 230−400 mesh ASTM). Elemental analysis was performed by M-H-W Laboratories (Phoenix, AZ). Anhydrous acetonitrile and triethylamine were freshly distilled from calcium hydride under an atmosphere of nitrogen and transferred via syringe or cannula. Bulk grade ethyl acetate (EtOAc) and Skellysolve B (referred to simply as "hexanes") were distilled before use. All purchased reagents were of reagent grade quality and were used without further purification. Penicillin G was purchased from Sigma. The wild-type class A TEM-1 β-lactamase from *E. coli* was purified according to literature methods.[14] All kinetic and spectral measurements were made on a Perkin-Elmer Lambda 3B or Hewlett-Packard 452 diode-array spectrophotometer. The enzyme assay and methods for determination of kinetic parameters were according to published procedures.[7]

(±)-Methyl 3-Hydroxybutanoate (7). A solution of 9.0 g (78 mmol) of methyl acetoacetate (**6**) in 300 mL of methanol was stirred at ice−water temperature under an atmosphere of nitrogen. Sodium borohydride (0.98 g, 26 mmol) was added to this solution, and the mixture was stirred for 30 min. Subsequently, the reaction was quenched by the addition of 100 mL of brine, the mixture was extracted with ether (3×), dried ($MgSO_4$), and filtered, and the solvent was evaporated in vacuo to afford 6.5 g (71%) of **7** as a colorless oil: ^1H NMR (300 MHz, $CDCl_3$) δ 1.23 (d, $J = 6.3$ Hz, 3H), 2.39−2.55 (m, 2H), 3.07 (br s, 1H), 3.71 (s, 3H), 4.14−4.27 (m, 1H); ^{13}C NMR (75 MHz, $CDCl_3$) δ 22.31, 42.64, 51.39, 63.97, 172.85.

(±)-Methyl 3-Hydroxy-2-[(1-hydroxy-1-phenyl)methyl]butanoate (8). *n*-Butyllithium (34 mL of a 2.5 M solution in hexanes, 85 mmol) was added to a stirred solution of 11.2 mL (85.4 mmol) of diisopropylamine in 34 mL of anhydrous THF at ice−water temperature under an atmosphere of argon. After 10 min of stirring, the solution was cooled to −78 °C and was stirred for an additional 5 min. This solution was charged with 5.0 g (42 mmol) of methyl 3-hydroxybutanoate (**7**) in 23 mL of anhydrous THF via cannula, and the resultant solution was stirred at the same temperature for 1 h. A solution of benzaldehyde (5.0 g, 47 mmol) in 23 mL of anhydrous THF was added to the mixture via cannula. The mixture was stirred for 3.5 h at −78 °C, at which time the reaction was quenched by the addition of saturated NH_4Cl, and was subsequently extracted with ether. The ether layer was washed with 1.0 M HCl, saturated $NaHCO_3$, and brine, dried ($MgSO_4$), and filtered, and the solvent was evaporated off to afford a yellow oil that was chromatographed on silica gel eluting with 30% EtOAc in hexanes to afford 7.0 g (74%) of **8** (four diastereomers) as a light yellow oil: R_f 0.30 (2:3, EtOAc:hexanes); IR (neat) 3445, 1725 cm^{-1}; ^1H NMR (300 MHz, $CDCl_3$) δ 1.21 (d, $J = 6.5$ Hz), 1.25 (d, $J = 6.6$ Hz), 1.29 (d, $J = 6.4$ Hz), 2.70−2.78 (m), 2.81−2.91 (m), 3.03 (d, $J = 5.0$ Hz), 3.28 (d, $J = 8.6$ Hz), 3.57 (s), 3.63 (s), 3.72 (s), 3.73−3.90 (m), 4.08−4.30 (m), 5.06−5.23 (m), 5.26 (t, $J = 5.5$ Hz), 7.26−7.43 (m); ^{13}C NMR (75 MHz, $CDCl_3$) δ 21.07, 21.61, 21.67, 22.13, 22.36, 42.50, 51.38, 51.66, 51.78, 56.98, 57.61, 58.94, 59.06, 60.65, 64.19, 65.71, 66.44, 67.03, 70.61, 71.49, 73.18, 73.97, 125.46, 125.93, 126.15, 126.54, 127.54, 127.74, 127.98, 128.21, 128.34, 128.38, 128.46, 141.62, 141.71, 171.90, 173.22, 173.58, 174.24; HRMS (FAB) calcd for $C_{12}H_{17}O_4$ (MH^+) 225.1127, found 225.1109.

(±)-*O*-Allyl 3-Hydroxy-2-(hydroxyphenyl)methylbutanohydroxamate (9). A stirred solution of 1.5 g (6.5 mmol) of the methyl ester **8** in 8.0 mL of THF was mixed with 7.2 mL of a 1.0 M NaOH solution at room temperature. The turbid solution was stirred for 2 h and was subsequently diluted with ether (10 mL). The layers were separated, and 0.92 g (8.4 mmol) of *O*-allyl hydroxylamine hydrochloride was added to the aqueous portion. The pH of the aqueous layer was adjusted to 4.5 using 1.0 M HCl, and 1.9 g (9.7 mmol) of EDC·HCl was added in four portions over a period of 1.5 h, while maintaining the pH of the solution at 4.5. The solution was extracted with EtOAc (3×). The combined organic layer was washed with 1.0 M HCl, 5% $NaHCO_3$ solution, and brine, dried (Na_2SO_4), and filtered, and the solvent was evaporated to afford 0.83 g (48%) of **9** as a white foam. The ^1H NMR was very complex due to the mixture of diastereomers, as well as the presence of hydroxamate and hydroximate forms. The mixture was used directly in the next step: IR (KBr) 3300 (broad), 1645 cm^{-1}; HRMS (FAB) calcd for $C_{14}H_{20}NO_4$ (MH^+) 266.1392, found 266.1392; MS (FAB) *m*/*z* 288 ($M + Na^+$).

General Procedure for the Preparation of β-Lactams 10−13. A stirred solution of 662 mg (2.49 mmol) of hydroxamate **9** in 20.0 mL of anhydrous THF was charged with 654 mg (2.49 mmol) of triphenylphosphine, followed by 574 mg (2.49 mmol) of di-*tert*-butyl azodicarboxylate (DBAD) at ice−water temperature under an atmosphere of nitrogen. The resulting solution was allowed to warm to room temperature and was allowed to stir for an additional 20 h. The solvent was evaporated, and the residue was chromatographed on silica gel eluting with 30% EtOAc in hexanes to afford 142 mg (23%) of **10** as a white solid, 77 mg (12%) of **11** as a colorless oil, 185 mg (30%) of **12** as a colorless oil, and 71 mg (12%) of **13** as a colorless oil.

(±)-*cis*-1-(Allyloxy)-3-[(hydroxyphenyl)methyl]-4-methyl-2-azetidinone (10): R_f 0.43 (1:1, EtOAc:hexanes); mp 86−87 °C (hexanes); IR (KBr) 3415 (OH), 1740 (CO) cm^{-1}; ^1H NMR (300 MHz, $CDCl_3$) δ 1.30 (d, $J = 6.4$ Hz, 3H), 2.86 (brs, 1H), 3.38 (dd, $J = 7.5$, 5.5 Hz, 1H), 3.93−4.04 (m, 1H), 4.38−4.52 (m, 2H), 4.90 (d, $J = 7.5$ Hz, 1H), 5.30−5.44 (m, 2H), 5.93−6.09 (m, 1H), 7.27−7.48 (m, 5H); ^{13}C NMR (75 MHz, $CDCl_3$) δ 13.73, 53.09, 56.54, 70.56, 77.22, 120.78, 126.98, 128.24, 128.59, 132.11, 141.15, 165.19; HRMS (FAB) calcd for $C_{14}H_{18}NO_3$ (MH^+) 248.1287, found 248.1285. Anal. Calcd for $C_{14}H_{17}NO_3$: C, 68.00; H, 6.93, N, 5.66. Found: C, 67.89; H, 7.12; N, 5.51.

(±)-*trans*-1-(Allyloxy)-3-[(hydroxyphenyl)methyl]-4-methyl-2-azetidinone (11): R_f 0.39 (1:1, EtOAc:hexanes); IR (neat) 3425 (OH), 1760 (CO) cm^{-1}; ^1H NMR (300 MHz, $CDCl_3$) δ 1.20 (d, $J = 6.0$ Hz, 3H), 2.88 (dd, $J = 6.9$, 1.8 Hz, 1H), 3.26 (d, $J = 2.7$ Hz, 1H), 3.68 (qd, $J = 6.0$, 2.1 Hz, 1H), 4.18−4.32 (m, 2H), 4.94 (dd, $J = 7.2$, 2.1 Hz, 1H), 5.18−5.32 (m, 2H), 5.78−5.95 (m, 1H), 7.25−7.44 (m, 5H); ^{13}C NMR (75 MHz, $CDCl_3$) δ 17.10, 56.47, 58.74, 72.30, 77.09, 120.81, 126.23, 128.18, 128.53, 132.04, 140.62, 164.54; HRMS (FAB) calcd for $C_{14}H_{18}NO_3$ (MH^+) 248.1287, found 248.1284.

(±)-*trans*-1-(Allyloxy)-3-(1-hydroxyethyl)-4-phenyl-2-azetidinone (12): R_f 0.38 (1:1, EtOAc:hexanes); IR (neat) 3450 (OH), 1765 (CO) cm^{-1}; ^1H NMR (300 MHz, $CDCl_3$) δ 1.35 (d, $J = 6.3$ Hz, 3H), 2.36 (br s, 1H), 2.85 (dd, $J = 6.0$, 2.4 Hz, 1H), 4.10−4.24 (m, 1H), 4.28−

(14) Zafaralla, G.; Manavathu, E. K.; Lerner, S. A.; Mobashery, S. *Biochemistry* **1992**, *31*, 3847.

4.44 (m, 2H), 4.72 (d, J = 2.1 Hz, 1H), 5.22−5.39 (m, 2H), 5.83−6.02 (m, 1H), 7.33−7.46 (m, 5H); ^{13}C NMR (75 MHz, $CDCl_3$) δ 21.35, 61.24, 63.28, 65.84, 77.05, 120.68, 126.61, 128.75, 128.92, 132.20, 136.64, 165.83; HRMS (FAB) calcd for $C_{14}H_{18}NO_3$ (MH^+) 248.1287, found 248.1289.

(±)-*cis*-1-(Allyloxy)-3-(1-hydroxyethyl)-4-phenyl-2-azetidinone (13): R_f 0.21 (1:1, EtOAc:hexanes); IR (neat) 3415 (OH), 1765 (CO) cm^{-1}; ^{1}H NMR (300 MHz, $CDCl_3$) δ 0.84 (d, J = 6.6 Hz, 3H), 2.41 (br s, 1H), 3.15 (dd, J = 8.4, 5.7 Hz, 1H), 3.65−3.80 (m, 1H), 4.38−4.55 (m, 2H), 5.05 (d, J = 5.7 Hz, 1H), 5.28−5.42 (m, 2H), 5.89−6.03 (m, 1H,), 7.32−7.46 (m, 5H); ^{13}C NMR (75 MHz, $CDCl_3$) δ 20.88, 56.60, 63.56, 64.76, 76.82, 120.76, 127.45, 128.85, 128.72, 132.15, 133.59, 166.09; HRMS (FAB) calcd for $C_{14}H_{18}NO_3$ (MH^+) 248.1287, found 248.1295.

(±)-*trans*-1-*N*-(Tosyloxy)-3-(1-hydroxyethyl)-4-phenyl-2-azetidinone (5). Triphenylphosphine (35 mg, 0.13 mmol), palladium diacetate (8 mg, 0.04 mmol), and pyrrolidine (31 μL, 0.37 mmol) were added to a stirred solution of 83 mg (0.34 mmol) of β-lactam **12** in 2.0 mL of anhydrous acetonitrile at room temperature under an atmosphere of argon for 1.5 h. The mixture was diluted with CH_2Cl_2 and was washed with 5% Na_2CO_3 (3×). The combined aqueous portion was washed with EtOAc, and it was acidified to pH 4.0 using 3.0 M HCl. The solution was washed with CH_2Cl_2 (3×), the combined organic layer was dried (Na_2SO_4) and filtered, and the solvent was evaporated to afford a yellow oil. The oil was dissolved in 2.0 mL of anhydrous CH_2Cl_2, and 70 mg (0.37 mmol) of *p*-toluenesulfonyl chloride and 50 μL (0.36 mmol) of triethylamine were added at room temperature. After 45 min of reaction time, the solvent was evaporated in vacuo to afford a brown oil. The oil was purified on a Chromatotron device (1 mm silica gel plate) eluting with 40% EtOAc in hexanes to afford 45 mg (37%) of **5** as a colorless oil: R_f 0.26 (2:3, EtOAc:hexanes); IR ($CDCl_3$) 3590, 1795 (CO) cm^{-1}; ^{1}H NMR (300 MHz, $CDCl_3$) δ 1.32 (d, J = 6.4 Hz, 3H), 1.90 (br s, 1H), 2.45 (s, 3H), 2.95 (dd, J = 5.3, 3.0 Hz, 1H), 4.08−4.21 (m, 1H), 4.86 (d, J = 3.0 Hz, 1H), 7.22−7.40 (m, 7H), 7.83 (d, J = 8.4 Hz, 2H); HRMS (FAB) calcd for $C_{18}H_{20}NO_5S$ (MH^+) 362.1062, found 362.1039.

Properties of the Rearranged Product 14: R_f 0.17 (2:3, EtOAc:hexanes); IR ($CDCl_3$) 3460, 1760 (CO) cm^{-1}; ^{1}H NMR (500 MHz, $CDCl_3$) δ 0.99 (d, J = 6.5 Hz, 3H), 2.37 (s, 3H), 3.75 (dd, J = 5.5, 1.0 Hz, 1H), 4.23 (pentet, J = 6.5 Hz, 1H), 5.29 (d, J = 8.0 Hz, 1H), 5.36 (br s, 1H), 7.11−7.19 (m, 3H), 7.24−7.35 (m, 4H), 7.55 (d, J = 8.5 Hz, 2H); ^{13}C NMR (125 MHz, $CDCl_3$) δ 20.29, 21.60, 62.98, 74.14, 84.68, 127.27, 127.75, 129.01, 129.68, 129.84, 132.97, 133.27, 145.11, 157.20; HRMS (FAB) calcd for $C_{18}H_{20}NO_5S$ (MH^+) 362.1062, found 362.1046.

Protein Crystallography. Orthorhombic crystals (380 × 200 × 200 μm^3) of the TEM-1 β-lactamase were prepared as previously described.[15] Soaking was performed at 4 °C during 4 days by adding the inhibitor as a racemic mixture (stock solution: 100 mM in 50% ammonium sulfate, 100 mM Na,K phosphate buffer, pH 7.8) to the mother liquor to a final concentration of 20 mM. The crystal was drawn up into a loop, flushed for few seconds with Paratone oil, and flash-cooled in a N_2 gas stream at 100 K.

Diffracted intensities were measured on the synchrotron beamline DW32 at LURE (Orsay, France). The wavelength was 0.975 Å, and the data were processed using MOSFLM (v. 5.40).[16] An 88% complete data set to 1.95 Å resolution (R_{sym} = 0.043; Table 1) was collected.

Refinement with CNS,[17] applying a bulk solvent correction, was carried out against all data (14192 reflections) except a randomly extracted set of structure factors used for calculation of the free R value.[18] The coordinates of the native TEM-1 enzyme were used as the initial model.[15] Rigid body refinement was performed in order to account for the variation in cell parameters between the native and the enzyme−inhibitor crystals. In each cycle of refinement, manual corrections using the program O[19] were followed by slow cooling using torsion angle molecular dynamics, energy minimization, and temperature factor refinement with maximum likelihood target function. Electrostatic energy terms were turned off. Water molecules were introduced as neutral oxygen atoms when they appeared as positive peaks at four standard deviations above the mean, in [$F_{obs} - F_{calc}$, Φ_{calc}] electron density maps. Hereafter, the slow-cooling scheme was abandoned for conventional refinement. Starting geometry of the inhibitor was obtained by optimization using DISCOVER (MSI). The final model was comprised of 2014 non-hydrogen protein atoms, including the covalently bound inhibitor, 349 water molecules, and one sulfate anion. The final R and free R values are 0.206 and 0.258 , respectively. The average B factors are 19.5 and 32.1 Å^2 for protein atoms and solvent, respectively (Table 1). Attempts were made to crystallographically refine the conformations of the inhibitor bound in the active starting from arbitrary initial conformations. For some of them, the ester oxygen atom was located in the oxyanion hole. In all cases, these independent refinements led to very similar final conformations of the bound inhibitor where the ester oxygen atom was located at 2.8 Å from Glu-166.

Acknowledgment. I.M. was the recipient of the Rumble and Heller Fellowships. The use of the Lizzadro Magnetic Resonance Center for the NMR studies at the University of Notre Dame is gratefully acknowledged. The work in France was funded in part by INSERM (CRE Contract 930612), the Regional Midi-Pyrenees (Contract 9200843), and CNRS (to J.P.S.). The work in the U.S. was supported by the National Institutes of Health and National Science Foundation (to S.M.) and Eli Lilly and Co. (to M.J.M.).

JA990400Q

(15) Jelsch, C.; Lenfant, F.; Masson, J. M.; Samama, J. P. *J. Mol. Biol.* **1992**, *223*, 377.

(16) Leslie, A. G. W. *Computational Aspects of Protein Crystal Data Analysis, Proceedings of the Daresbury Study Weekend*; SERC, Daresbury Laboratory: Warrington, U.K., 1987; pp 39−50.

(17) Brünger, A. T.; Adams, P. A.; Clore, M. G.; DeLano, W. L.; Gros, P.; Grosse-Kunstieve, R. W.; Jiang, J. S.; Kuszewski, J.; Nilges, M.; Pannu, N. S.; Read, R.; Rice, L. M.; Simonson, T.; Warren, G. L. *Acta Crystallogr.* **1998**, *D54*, 905.

(18) Brünger, A. T. *Nature* **1992**, *355*, 472.

(19) Jones, T. A.; Zou, J. Y.; Cowan, S. W.; Kjeldgaard, M. *Acta Crystallogr.* **1991**, *A47*, 110.